Biomedical Instrumentation

Prof. Dr. Nizamettin AYDIN

naydin@yildiz.edu.tr
naydin@ieee.org
http://www.yildiz.edu.tr/~naydin

1

Chemical Biosensors

Table 10.1 Critical-Care Analytes and Their Normal Ranges in Blood

Blood Gases and Related Parameters		Electrolytes		Metabolites	
P_{O_2}	80–104 mm Hg	Na^+	135–155 mmol/l	Glucose	70–110 mg/100 ml
P_{CO_2}	33–48 mm Hg	K^+	3.6–5.5 mmol/l	Lactate	3–7 mg/100 ml
pH	7.31–7.45	Ca^{2+}	1.14–1.31 mmol/l	Creatinine	0.9–1.4 mg/100 ml
Hematocrit	40–54%	Cl^-	98–109 mmol/l	Urea	8–26 mg/100 ml
Total hemoglobin	13–18 g/100 ml				
O_2-saturation	95–100%				

SOURCE: M. E. Collison and M. E. Meyerhoff, "Chemical sensors for bedside monitoring of critically ill patients," *Anal. Chem.*, 1990, 62, 425A–437A.

Table 10.1

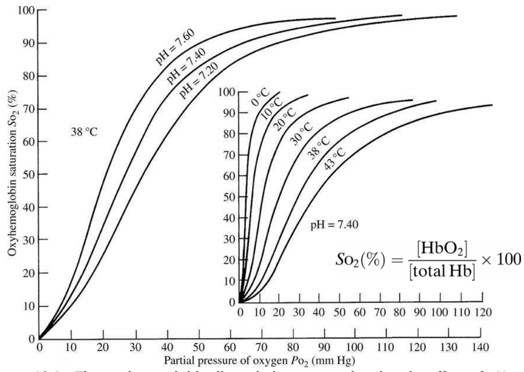

Figure 10.1 The oxyhemoglobin dissociation curve, showing the effect of pH and temperature on the relationship between *S*O2 and *P*O2.

Table 10.2 Examples of Arterial Blood Gases in Different Clinical Situations

Example	P_{CO_2}, mm Hg	pH	P_{O_2}, mm Hg	Interpretation	Likely Causes	Therapy
1	40 ± 3	7.40 ± 0.03	90 ± 5	Normal blood gas		None
2	44 ± 3	7.37 ± 0.03	88 ± 5	Normal blood gas while asleep		
3	22	7.57	106	Hyperventilation	Anxiety	None
4	68	7.10	58	Hypoventilation	Central nervous system depression; blockage of upper airway	Mechanical ventilation; relieve the cause
5	58	7.21	39	Hypoventilation and hypoxemia	Pneumonia; small-airway obstruction; severe asthma	Oxygen; bronchodilators; mechanical ventilation
6	61	6.99	29	Combined respiratory and metabolic acidosis and hypoxemia	Birth asphyxia; near-drowning	Oxygen; mechanical ventilation; buffers?
7	60	7.37	106	Chronic respiratory acidosis with metabolic compensation; patient is receiving supplemental oxygen	Patient has chronic lung disease and is on oxygen	Treat chronic disease; no additional therapy may be necessary
8	29	7.31	106	Metabolic acidosis with respiratory compensation	Diabetic; ketoacidosis; dehydration	Treat the cause; buffers?

SOURCE: B. G. Nickerson and F. Monaco, "Carbon dioxide electrodes, arterial and transcutaneous," in J. G. Webster (ed.), Encyclopedia of Medical Devices and Instrumentation. New York: Wiley, 1988, pp. 564–569.

Table 10.2

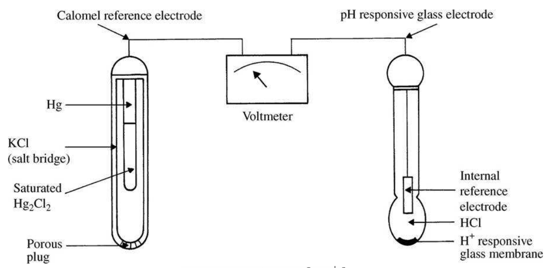

$$\mathrm{pH} = -\log_{10}[\mathrm{H}^+]$$

Figure 10.2 pH electrode (From R. Hicks, J. R. Schenken, and M. A. Steinrauf, Laboratory Instrumentation. Hagerstown, MD: Harper & Row, 1974. Used with permission of C. A. McWhorter.)

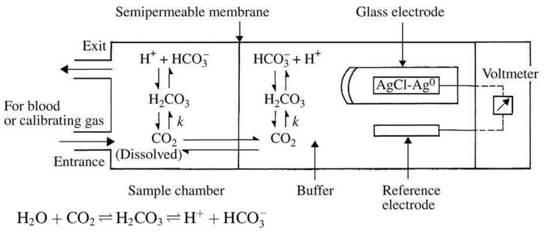

$$H_2O + CO_2 \rightleftharpoons H_2CO_3 \rightleftharpoons H^+ + HCO_3^-$$

$$[CO_2] = a(P\mathrm{CO}_2)$$

$$\log[H^+] + \log[HCO_3^-] - \log k - \log a - \log P\mathrm{CO}_2 = 0$$

$$\mathrm{pH} = \log[HCO_3^-] - \log k - \log a - \log P\mathrm{CO}_2$$

Figure 10.3 ***P*CO2 electrode (From R. Hicks, J. R. Schenken, and M. A. Steinrauf, Laboratory Instrumentation. Hangerstown, MD: Harper & Row, 1974. Used with permission of C. A. McWhorter.)**

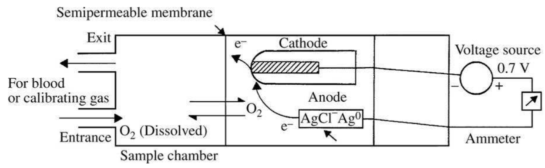

$$O_2 + 2H_2O + 4e^- \rightarrow 2H_2O_2 + 4e^- \rightarrow 4OH^-$$

$$4OH^- + 4KCl \rightarrow 4KOH + 4Cl^-$$

$$4Ag + 4Cl^- \rightarrow 4AgCl + 4e^-$$

Figure 10.4 ***P*O2 electrode (From R. Hicks, J. R. Schenken, and M. A. Steinrauf, Laboratory Instrumentation. Hangerstown, MD: Harper & Row, 1974. Used with permission of C. A. McWhorter.)**

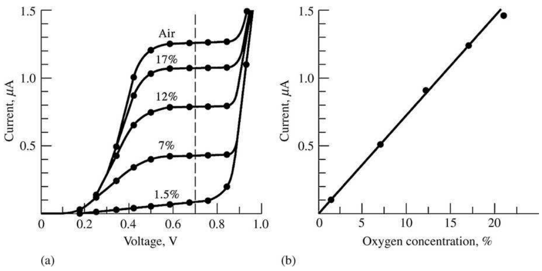

Figure 10.5 (a) Current plotted against polarizing voltage for a typical *P*O2 electrode for the percents O2 shown. (b) Electrode operation with a polarizing voltage of 0.68 V gives a linear relationship between current output and percent O2.

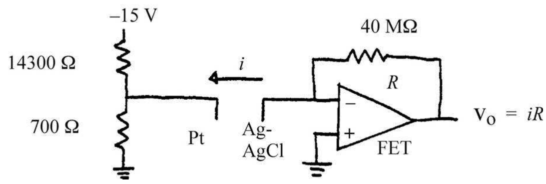

Figure E10.3 From a –15 V power supply use a 14300 Ω and 700 Ω resistor voltage divider to yield –0.7 V to bias the Pt electrode. Feed the Ag/AgCl electrode output into an FET current-to-voltage converter with a feedback resistor = *V*/*I* = 10 V/250 nA = 40 MΩ.

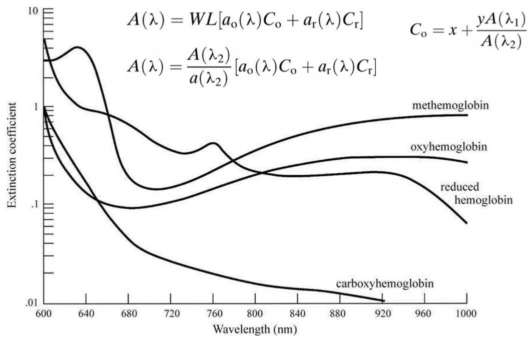

$$A(\lambda) = WL[a_o(\lambda)C_o + a_r(\lambda)C_r]$$

$$C_o = x + \frac{yA(\lambda_1)}{A(\lambda_2)}$$

$$A(\lambda) = \frac{A(\lambda_2)}{a(\lambda_2)}[a_o(\lambda)C_o + a_r(\lambda)C_r]$$

Figure 10.6 Absorptivities (extinction coefficients) in L/(mmol·cm) of the four most common hemoglobin species at the wavelengths of interest in pulse oximetry. (Courtesy of Susan Manson, Biox/Ohmeda, Boulder, CO.)

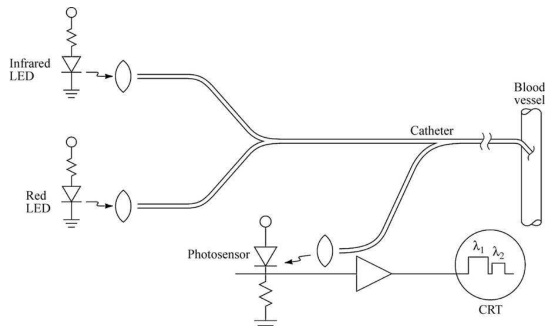

Figure 10.7 The oximeter catheter system measures oxygen saturation in vivo, using red and infrared light emitting diodes (LFDs) and a photosensor. The red and infrared LEDs are alternately pulsed in order to use a single photosensor.

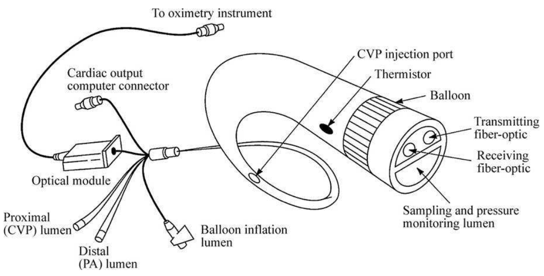

Figure 10.8 The catheter used with the Abbott Opticath Oximetry System transmits light to the blood through a transmitting optical fiber and returns the reflected light through a receiving optical fiber. The catheter is optically connected to the oximetry processor through the optical module. (From Abbott Critical Care Systems. Used by permission.)

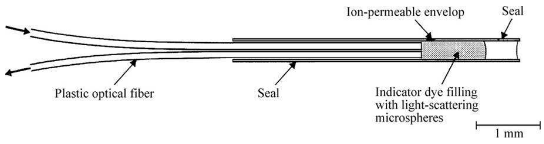

Figure 10.9 A reversible fiber-optic chemical sensor measures light scattered from phenol red indicator dye to yield pH. [From J. I. Peterson, "Optical sensors," in J. G. Webster (ed.), Encyclopedia of Medical Devices and Instrumentation. New York: Wiley, 1988, pp. 2121–2133. Used by permission.]

$$R = k \times 10^{\left[-C/\left(10^{-\Delta}+1\right)\right]}$$

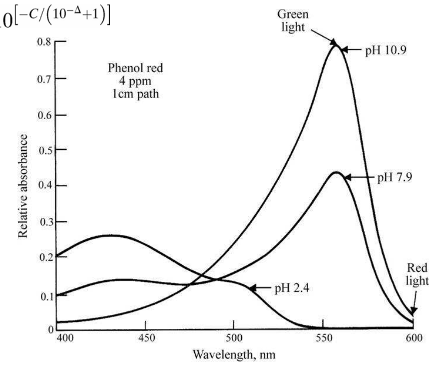

Figure 10.10 The plot of absorbance against wavelength of phenol red (base form) increases with pH for green light but is constant for red light.

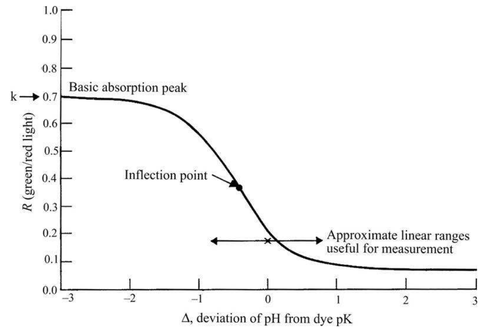

Figure 10.11 The ratio (*R*) of green to red light transmitted through phenol red for basic and acidic forms of the dye. Δ = deviation of pH from dye pK. (From J. I. Peterson, S. R. Goldstein, and R. V. Fitzgerald, "Fiber-optic pH probe for physiological use." *Anal. Chem.*, 1980, 52, 864–869. Used by permission.)

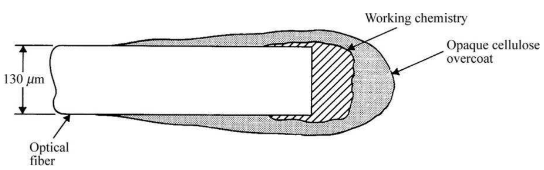

Figure 10.12 A single-fiber intravascular blood-gas sensor excites fluorescent dye at one wavelength and detects emission at a different wavelength. The following modifications are made to the sensor tip: pH: Chemistry—pH-sensitive dye bound to hydrophilic matrix. *P*CO2: Chemistry—Bicarbonate buffer containing pH-sensitive dye with silicone. *P*O2: Chemistry—Oxygen-sensitive dye in silicone. (From J. L. Gehrich, D.W. Lübbers, N. Optiz, D. R. Hansmann, W. E. Miller, J. K. Tusa, and M. Yafuso, "Optical fluorescence and its application to an intravascular blood gas monitoring system," *IEEE Trans. Biomed. Eng.*, 1986, BME-33, 117–132. Used by permission.)

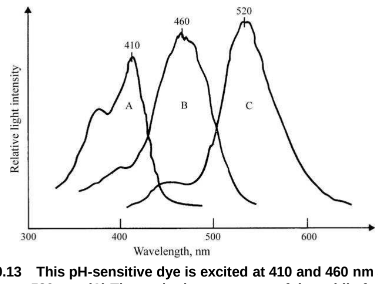

Figure 10.13 This pH-sensitive dye is excited at 410 and 460 nm and fluoresces at 520 nm. (A) The excitation spectrum of the acidic form of the dye; (B) the excitation spectrum of the basic form of the dye; (C) the emission spectrum of the acidic and basic forms of the dye. (From J. I. Gehrich, D. W. Lübbers, N. Opitz, D. R. Hansmann, W. W. Miller, J. K. Tusa, and M. Yafuso, "Optical fluorescence and its application to an intravascular blood gas monitoring system," *IEEE Trans. Biomed. Eng.*, 1986, BME-33, 117–132. Used by permission.)

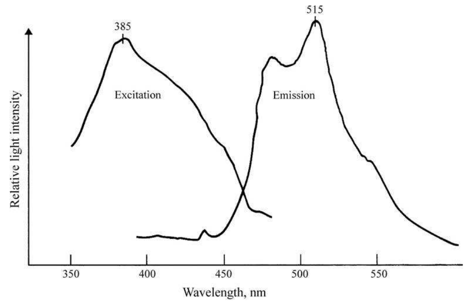

Figure 10.14 The emission spectrum of oxygen-sensitive dye can be separated from the excitation spectrum by a filter. (From J. L. Gehrich, D. W. Lübbers, N. Opitz, D. R. Hansmann, W. W. Miller, J. K. Tusa, and M. Yafuso, "Optical fluorescence and its application to an intravascular blood gas monitoring system," *IEEE Trans. Biomed. Eng*., 1986, BME-33, 117–132. Used by permission.)

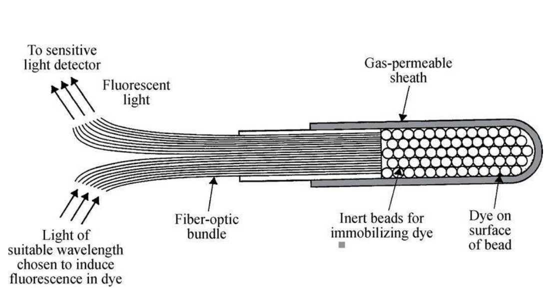

Figure 10.15 In a fiber-optic oxygen sensor, irradiation of dyes causes fluorescence that decreases with *P*O2. [From R. Kocache, "Oxygen analyzers." in J. G. Webster (ed.), Encyclopedia of Medical Devices and Instrumentation. New York: Wiley, 1988, pp. 2154–2161. Used by permission.]

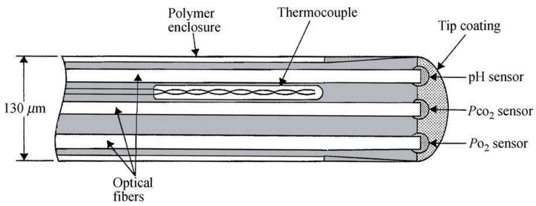

Figure 10.16 An intravascular blood-gas probe measure pH, *P*CO2, and *P*O2 by means of single fiber-optic fluorescent sensors. (From J. L. Gehrich, D. W. Lübbers, N. Optiz, D. R. Hansmann, W. W. Miller, J. K. Tusa, and M. Yafuso, "Optical fluorescence and its application to an intravascular blood gas monitoring system," *IEEE Trans. Biomed. Eng*., 1986, BME-33, 117–132. Used by permission.)

Figure 10.17 (a) In a chemically sensitive field-effect transistor, the ion-selective membrane modulates the current between the source and the drain. (b) A stretched ISFET maximizes the spacing between the "wet" sample region and the electric connections. (Part (b) from P. Rolfe, "In vivo chemical sensors for intensive-care monitoring," *Med. Biol. Eng. Comput*., 1990, 28. Used by permission.)

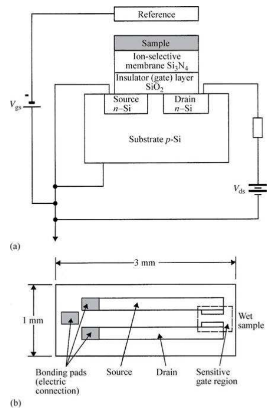

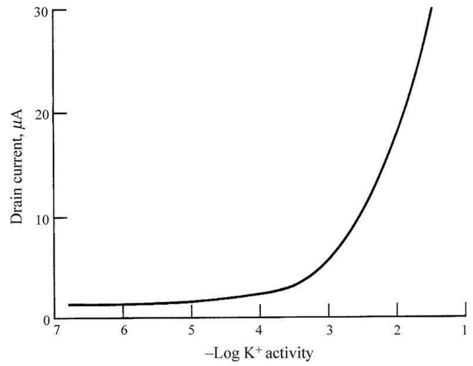

Figure 10.18 Dependence of current on potassium ion activity for a potassium ion-sensitive field-effect transistor.

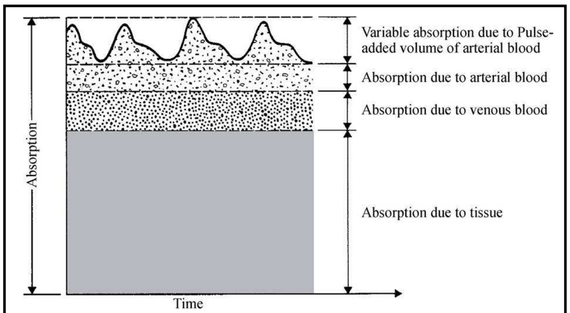

Figure 10.19 The pulse oximeter analyzes the light absorption at two wavelengths of only the pulse-added volume of oxygenated arterial blood. [From Y. M. Mendelson, "Blood gas measurement, transcutaneous," in J. G. Webster (ed.), *Encyclopedia of Medical Devices and Instrumentation*. New York: Wiley, 1988, pp. 448–459. Used by permission.]

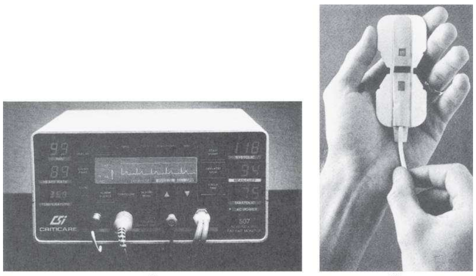

Figure 10.20 (a) Noninvasive patient monitor capable of measuring ECG, noninvasive blood pressure (using automatic oscillometry), respiration (using impedance pneumography), transmission pulse oximetry, and temperature. (From Criticare Systems, Inc. Used by permission.) (b) Disposable transmission *S*O2 sensor in open position. Note the light sources and detector, which can be placed on each side of the finger. (From Datascope Corporation. Used by permission.)

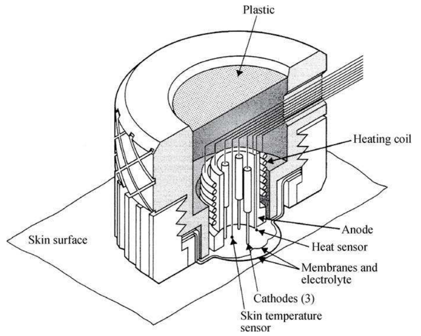

Figure 10.21 Cross-sectional view of a transcutaneous oxygen sensor. Heating promotes arterialization. (From A. Huch and R. Huch, "Transcutaneous, noninvasive monitoring of *P*O2," *Hospital Practice*, 1976, 6, 43–52. Used by permission.)

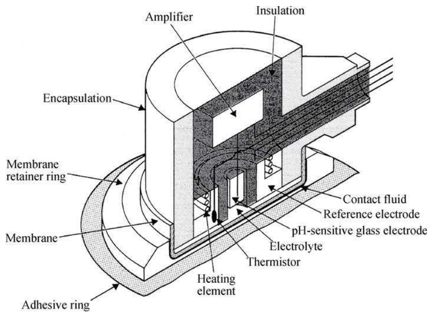

Figure 10.22 Cross-sectional view of a transcutaneous carbon dioxide sensor. Heating the skin promotes arterialization. (From A. Huch, D. W. Lübbers, and R. Huch, "Patientenuberwachung durch transcutane *P*co2 Messung bei gleiechzeiliger koutrolle der relatiuen lokalen perfusion," *Anaesthetist*, 1973, 22, 379. Used by permission.)

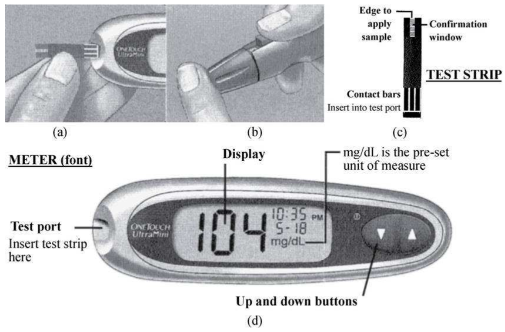

Figure 10.23 (a) A test strip is inserted into the meter. (b) A lance is released to lance the skin less than 1 mm. (c) The 1 μL blood sample is applied to the end of the test strip and drawn into it by capillary action. (d) 5 s later the meter displays the blood glucose in mg/dL. From www.LifeScan.com.

Figure 10.24 (a) In the enzyme electrode, when glucose is present it combines with O2, so less O2 arrives at the cathode. (b) In the dual-cathode enzyme electrode, one electrode senses only O2 and the difference signal measures glucose independent of O2 fluctuations. (From S. J. Updike and G. P. Hicks, "The enzyme electrode, a miniature chemical transducer using immobilized enzyme activity," *Nature*, 1967, 214, 986–988. Used by permission.)

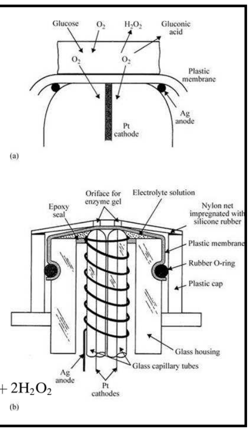

$$\text{Glucose} + 2H_2O + O_2 \xrightarrow{\text{glucose oxidase}} \text{Gluconic Acid} + 2H_2O_2$$

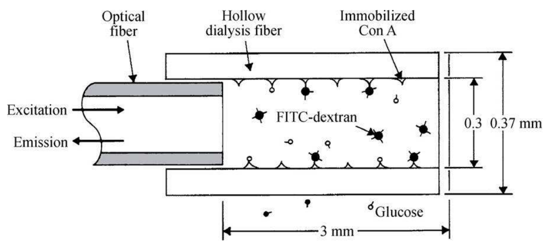

Figure 10.25 The affinity sensor measures glucose concentration by detecting changes in fluorescent light intensity caused by competitive binding of a fluorescein-labeled indicator. (From J. S. Schultz, S. Manouri, *et al.*, "Affinity sensor: A new technique for developing implantable sensors for glucose and other metabolites," *Diabetes Care*, 1982 5, 245–253. Used by permission.)

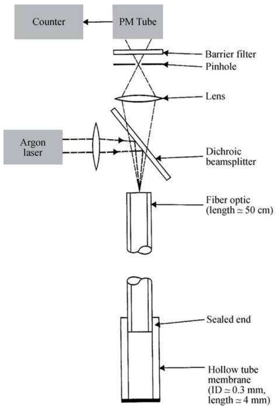

Figure 10.26 The optical system for a glucose affinity sensor uses an argon leaser and a fiber-optic catheter. (From J. S. Schulz, S. Manouri, *et al*., "Affinity sensor: A new technique for developing implantable sensors for glucose and other metabolites," *Diabetes Care*, 1982, 5, 245–253. Used by permission.)

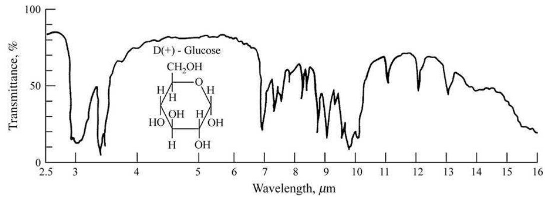

Figure 10.27 The infrared absorption spectrum of anhydrous D-glucose has a strong absorption peak at 9.7 mm. (From Y. M. Mendelson, A. C. Clermont, R. A. Peura, and B. C. Lin, "Blood glucose measurement by multiple attenuated total reflection and infrared absorption spectroscopy," *IEEE Trans. Biomed Eng*., 1990, 37, 458–465. Used by permission.)

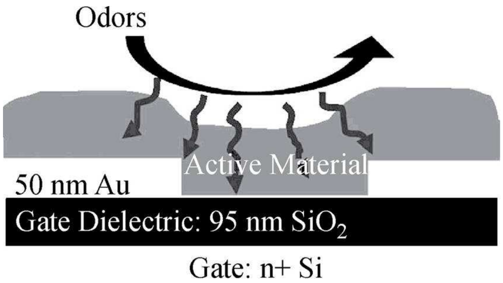

Figure 10.28 A printed organic thin-film transistor senses volatile organic compounds to yield an affordable electronic nose. A 2.5 nm chrome adhesion layer and 50 nm thick gold source and drain pads are thermally evaporated onto 95 nm of thermally grown wet oxide. The active material is spun cast or drop cast. From J. B. Chang, V. Liu, V. Subramanian, K. Sivula, C. Luscombe, A. Murphy, J. Liu, and J. M. J. Fréchet, Printable polythiophene gas sensor array for low-cost electronic noses, *J. Appl, Phys*., 2006, 100, 014506.

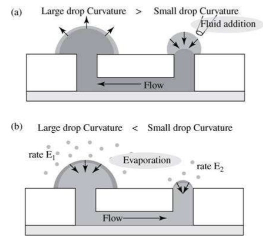

Figure 10.29 Schematic of a passive pumping device. A. Flowing fluid in the channel is effectuated by adding a drop to the port opposing the large drop. The subsequent increase of pressure due to the small curvature of the added drop provokes its flow towards the large drop until curvatures match. This happens in seconds to minutes. B. During the storage of the channel, as evaporation occurs both at the large and small drop, a decrease in volume will provoke more decrease in curvature in the small drop, and thus an unbalance of pressure in its favor. A flow will be generated from the large to the small drop, thus ensuring constant wetting of the port. From Berthier, E., J. Warrick, H. Yu and D. J. Beebe, Managing evaporation for more robust microscale assays. Part 2. Characterization of convection and diffusion for cell biology, *Lab Chip*, 2008, 8, 860–864. Reproduced by permission of The Royal Society of Chemistry.